Biochimica et Biophysica Acta 1848 (2015) 643–653

Contents lists available at ScienceDirect

Biochimica et Biophysica Acta

journal homepage: www.elsevier.com/locate/bbamem

Hydrogel-assisted functional reconstitution of human P-glycoprotein (ABCB1) in giant liposomes

Kim S. Horger [a,1], Haiyan Liu [b,1], Divya K. Rao [b], Suneet Shukla [c], David Sept [b,d], Suresh V. Ambudkar [c], Michael Mayer [a,b,*]

[a] Department of Chemical Engineering, University of Michigan, 2300 Hayward Street, Ann Arbor, MI 48109, USA
[b] Department of Biomedical Engineering, University of Michigan, 1101 Beal Avenue, Ann Arbor, MI 48109, USA
[c] Laboratory of Cell Biology, Center for Cancer Research, National Cancer Institute, National Institutes of Health, 37 Convent Drive, Bethesda, MD 20814, USA
[d] Center for Computational Medicine and Bioinformatics, University of Michigan, 2800 Plymouth Road, Ann Arbor, MI 48109, USA

ARTICLE INFO

Article history:
Received 18 March 2014
Received in revised form 17 September 2014
Accepted 20 October 2014
Available online 4 November 2014

Keywords:
Liposome
Proteoliposome
P-glycoprotein
Chloride ion channel
Transport rate constant
Permeability

ABSTRACT

This paper describes the formation of giant proteoliposomes containing P-glycoprotein (P-gp) from a solution of small proteoliposomes that had been deposited and partially dried on a film of agarose. This preparation method generated a significant fraction of giant proteoliposomes that were free of internalized vesicles, making it possible to determine the accessible liposome volume. Measuring the intensity of the fluorescent substrate rhodamine 123 (Rho123) inside and outside these giant proteoliposomes determined the concentration of transported substrates of P-gp. Fitting a kinetic model to the fluorescence data revealed the rate of passive diffusion as well as active transport by reconstituted P-gp in the membrane. This approach determined estimates for the membrane permeability coefficient (P_s) of passive diffusion and rate constants of active transport (k_T) by P-gp as a result of different experimental conditions. The P_s value for Rho123 was larger in membranes containing P-gp under all assay conditions than in membranes without P-gp indicating increased leakiness in the presence of reconstituted transmembrane proteins. For P-gp liposomes, the k_T value was significantly higher in the presence of ATP than in its absence or in the presence of ATP and the competitive inhibitor verapamil. This difference in k_T values verified that P-gp was functionally active after reconstitution and quantified the rate of active transport. Lastly, patch clamp experiments on giant proteoliposomes showed ion channel activity consistent with a chloride ion channel protein that co-purified with P-gp. Together, these results demonstrate several advantages of using giant rather than small proteoliposomes to characterize transport properties of transport proteins and ion channels.

1. Introduction

Giant liposomes are useful models to study diffusion or transport of solutes across biological membranes since their interiors are isolated from the surrounding fluid by a self-enclosing membrane and can be observed individually by optical microscopy [1–5]. To study protein-mediated transport, functional transmembrane proteins must be incorporated into the membrane of giant liposomes that consist of a single lipid bilayer (giant unilamellar vesicle, GUV). Few methods exist for the production of such giant proteoliposomes with active ion channels or transporter proteins due to the sensitive and fragile nature of many transmembrane proteins and GUVs [6–10]. In addition, existing methods can lead to giant proteoliposomes that enclose many smaller liposomes making it difficult to determine the accessible volume inside these liposomes.

Many of the current methods for forming giant proteoliposomes are variations of the classic protocols of gentle hydration or electroformation, but with a carefully executed, gentle dehydration step to prevent denaturation of the proteins [7,11–19]. To this end, most methods involve reconstituting transmembrane proteins into small unilamellar vesicles (SUVs), and then partially drying the SUVs into a film under controlled conditions before rehydrating the film in an aqueous solution [15–18]. Chemicals such as carbohydrates or ethylene glycol may be added to prevent complete dehydration [16–19]. Additionally, formation of giant proteoliposomes using water-in-oil droplet transfer technique [20] or by fusion of small proteoliposomes with pre-formed GUVs [15,21,22] has also been reported. These methods, however, can have limitations with regard to their final lipid or protein composition [6,7,23]. Alternatively, Dezi et al. reported a method to directly incorporate proteins from detergents into liposomes [8].

Abbreviations: GUV, giant unilamellar vesicle; $I_{in,t}$, fluorescence intensity inside liposome at time, t; $I_{out,t}$, fluorescence intensity outside liposome at time, t; k_T, rate constant of active transport; NPPB, 5-Nitro-2-(3-phenylpropylamino)benzoic acid; P-gp, P-glycoprotein; P_s, membrane permeability; r, radius of liposome; Rho123, rhodamine 123; SUV, small unilamellar vesicle

* Corresponding author at: Department of Chemical Engineering and Department of Biomedical Engineering, University of Michigan, 1101 Beal Avenue, Ann Arbor, MI 48109, USA. Tel.: +1 734 763 4609.
E-mail address: mimayer@umich.edu (M. Mayer).
[1] Both authors contributed equally to this work.

http://dx.doi.org/10.1016/j.bbamem.2014.10.023
0005-2736/

Previously, we described the use of a hybrid film of dried agarose to assist formation of protein-free GUVs in solutions of physiologic ionic strength [24]. Since the film of agarose provided partial hydration, we hence hypothesized that such a film of agarose might be useful for reconstituting membrane proteins into giant proteoliposomes. The Malmstadt group has recently reported an elegant approach to form giant proteoliposomes that used direct dilution of detergent-solubilized membrane proteins in combination with lipid hydration from an agarose film [25,26]. Here, we explored whether hydrogel films might also be useful for the formation of giant proteoliposomes from small proteoliposomes since small proteoliposomes are one of the most commonly used membrane protein preparations. To this end, we reconstituted the human multidrug resistance-linked ABCB1 transporter, commonly known as P-glycoprotein (P-gp) [27], in GUVs using this method. P-gp, a member of ATP-binding cassette (ABC) family, contains two ATP binding domains and 12 transmembrane α-helices [28–32]. By hydrolyzing ATP, P-gp actively effluxes a broad range of hydrophobic or amphipathic molecules, leading to the development of multi-drug resistance (MDR) of cancer cells [28–32]. The ability to assay P-gp activity for biophysical studies as well as drug screening and development is of interest due to the role of P-gp in the blood–brain barrier and in cancer cells [29–32].

Attempts to study P-gp activity thus far have been restricted primarily to cell-based assays. Consequently, measured transport rates, with or without potential modulators, can be complicated by the presence of other transporter proteins and cellular constituents [31–33]. Liposome-based studies using purified P-gp have been conducted using primarily small proteoliposomes due, in part, to the difficulty of incorporating P-gp into giant proteoliposomes [6,34–36]. Sasaki et al. [37] recently described a transport assay using commercially available giant proteoliposomes (diameter < 3 μm) containing reconstituted P-gp. The fluorescent substrate was restricted to sub-μM concentrations because the signal inside the liposomes would otherwise be affected by accumulation of fluorescent substrate on or in the membrane.

In the work presented here, we reconstituted purified P-gp and then assessed its functionality by (i) measuring the rate of ATP hydrolysis, and (ii) determining the passive and active transport rates by a fluorescence flux assay, and performed patch clamp experiments of a putative chloride channel that co-purified with P-gp [38]. We introduce a straightforward model for the transport of the fluorescent substrate in and out of liposomes. This model makes it possible to distinguish between passive diffusion and active transport of a fluorescent molecule. This distinction is important because reconstitution of transmembrane proteins typically increases passive diffusion through liposome membranes [39] while the transport rate of efflux pumps and other transporter proteins is typically relatively slow [27]. A model that cannot distinguish between active and passive transport may therefore be dominated by the passive term and hence be inadequate for quantitative analysis.

2. Materials and methods

Chemicals were purchased from Sigma-Aldrich (St. Louis, MO), except when noted otherwise.

2.1. Isolation of crude membranes from P-gp-expressing high five insect cells

We prepared crude membranes from High Five insect cells infected with recombinant baculovirus carrying the 6 × His-tagged human MDR1 cDNA as described previously [40]. We incubated cells on ice for 45 min in a lysis buffer containing 50 mM trizma hydrochloride (Tris–HCl), pH 7.5, 50 mM mannitol, 2 mM ethylene glycol tetraacetic acid (EGTA), 2 mM dithiothreitol (DTT), 1 mM 4-(2-aminoethyl) benzenesulfonyl fluoride (AEBSF), and 1% (w/v) aprotinin (Roche Diagnostics, Indianapolis, IN) and subsequently disrupted the cells using a Dounce homogenizer (30 strokes with pestle A). We removed undisrupted cells and nuclear debris by centrifugation at 500 ×*g* for 10 min. We diluted the supernatant 2-fold in resuspension buffer containing 50 mM Tris–HCl (pH 7.5), 300 mM mannitol, 1 mM EGTA, 1 mM DTT, 1 mM AEBSF, and 1% (w/v) aprotinin. We collected the membranes by centrifugation for 60 min at 100,000 ×*g* and resuspended the pellet in resuspension buffer containing 10% (v/v) glycerol. We stored the membranes in small aliquots at −70 °C. The Amido Black protein method described by Schaffner and Weissmann [41] revealed the protein content of each preparation with bovine serum albumin (BSA) as a standard.

2.2. Solubilization of P-gp

We solubilized membranes prepared from High Five insect cells using octyl β-D-glucopyranoside as described [42–44] with modifications. We resuspended crude membranes at a concentration of 2.0 mg/mL in a buffer containing: 20 mM Tris–HCl (pH 8.0), 20% (v/v) glycerol, 150 mM NaCl, 2 mM β-mercaptoethanol, 2.0% (w/v) octyl glucoside, 1.5 mM $MgCl_2$, 1 mM AEBSF, 2 μg/mL pepstatin, 2 μg/mL leupeptin, 1% (w/v) aprotinin and a 0.4% (w/v) lipid mixture consisting of *Escherichia coli* bulk phospholipid, phosphatidylcholine, phosphatidylserine, and cholesterol (all from Avanti Polar Lipids, Alabaster, AL) at 60:17.5:10:12.5 (w/w), respectively [42,45]. After 20 min of incubation on ice, we removed insoluble material by centrifugation at 100,000 ×*g* for 1 h. The supernatant, which we call detergent extract, contained the solubilized P-gp.

2.3. Purification of P-gp by metal affinity chromatography

We purified P-gp as previously described [42–44] with modifications. Briefly, we incubated the detergent extract (10 mg of protein) in the presence of 2 mM imidazole (final concentration) for 30 min at 4 °C on a rotary shaker with 0.5 mL of 50% (w/v) Talon metal affinity resin in non-buffered 20% ethanol (Clontech, Mountain View, CA). The resin was prewashed once with buffer A composed of 20 mM Tris–HCl (pH 8.0), 100 mM NaCl, 20% (v/v) glycerol, 2.5 mM β-mercaptoethanol, 1.25% (w/v) octyl glucoside, 1 mM $MgCl_2$, 1 mM AEBSF, 2 μg/mL pepstatin, 2 μg/mL leupeptin, 1% (w/v) aprotinin and a 0.1% (w/v) lipid mixture (same composition as the solubilization reaction). We pelleted the metal affinity beads by centrifugation for 5 min at 500 ×*g* and washed twice by resuspending and incubating in 10 mL of buffer A at 4 °C for 10 min on a rotary shaker. We resuspended the beads in 1 mL of buffer A and transferred them to a 4 mL disposable column (Bio-Rad, Hercules, CA). After being washed twice in 5 mL of buffer A containing 500 mM KCl, we eluted the proteins stepwise in 2 mL each of buffer B (same as buffer A except with 20 mM Tris–HCl at pH 6.8 instead of at pH 8.0) containing 10, 100, and 200 mM imidazole. We concentrated the fractions eluted from the column using Centriprep-50 concentrators (Amicon, Beverly, MA) and stored in aliquots at −70 °C. We analyzed the protein content of the purified sample by the Amido Black protein method and performed sodium dodecyl sulfate polyacrylamide gel electrophoresis (SDS-PAGE) and immunoblot analysis (Fig. S3) as previously described [41,42]. We estimate the purity of this P-gp preparation to be 70 to 80%.

2.4. Reconstitution of P-gp into small proteoliposomes

We reconstituted P-gp into small proteoliposomes by the detergent-dilution method as previously described [42–44]. Briefly, we used 160–250 μg of purified and concentrated P-gp. We mixed the protein sample with 4–5 mg of tip sonicated phospholipid mixture (same composition as the solubilization reaction at 50 mg/mL in 50 mM Tris–HCl, pH 7.4), 1.25% octylglucoside, and 50 mM Tris–HCl, pH 7.4, in a final volume of 1 ml [42,45]. We incubated the mixture for 20 min on ice and formed proteoliposomes or control liposomes (prepared in the same way but without protein) at 23–25 °C by a 1:25 dilution into buffer C composed of 50 mM Tris–HCl, pH 7.4, 1 mM DTT, and 1× protease inhibitor cocktail (Roche Diagnostics, Indianapolis, IN). We concentrated

the proteoliposomes or liposomes by centrifugation at 100,000 ×*g*, washed once, and resuspended in 150 μL of buffer C containing protease inhibitors and 2.5 mM $MgCl_2$. The 1:25 dilution in buffer C reduces the concentration of the detergent below its critical micelle concentration (CMC) value, thereby breaking up the protein–detergent micelles and facilitating the incorporation of P-gp into unilamellar vesicles in the inside-out configuration [42–44].

2.5. Formation of giant proteoliposomes

To form giant proteoliposomes from small proteoliposomes, we extended a technique that we described previously for the formation of protein-free liposomes [24]. We prepared ~10 mL of a solution of 1% (w/w) ultra-low melting agarose (Type IX-A from Sigma-Aldrich, St. Louis, MO) in deionized water by boiling the suspension of agarose powder and water twice in a microwave with gentle agitation between heating. After the solution cooled to room temperature, we reheated it for 10 s in a microwave and immediately dip-coated one side of a cover glass (24 × 50 × 0.15 mm, from Fisher Scientific, Rochester, NY) in the agarose solution. We placed the cover glass with the agarose-coated side facing upward on a temperature-controlled hot plate (Barnstead Intl, Dubuque, IA) and covered the glass with the lid from a Petri dish set at an angle to allow water vapor to escape while preventing dust from settling onto the agarose film. The cover glass remained on the hot plate with the temperature set to 40 °C until the solution appeared dry (typically ~20 min).

After the agarose solution dried into a clear film, we hand-cut a rectangular frame of poly-dimethylsiloxane (PDMS) (Sylgard 184 Silicone, Dow Corning Corporation, Midland, MI) to the size of the cover glass and placed the PDMS frame onto the agarose-coated side of the cover glass. Using a pipette, we dispersed 150 μL of the solution containing small proteoliposomes in small droplets (~10 μL each) onto the dried film of agarose while trying to cover the entire surface enclosed within the PDMS frame. We dragged the pipette tip over the tops of the droplets until they coalesced into a single film of solution while taking care not to disturb the underlying agarose film. We placed the lid from a Petri dish set at an angle over the cover glass and kept the cover glass undisturbed overnight at room temperature, or until the solution appeared dry. In the last few trials, we applied a vacuum (approximately −500 mm Hg) to shorten the drying time to less than 2 h.

When the solution of small liposomes appeared dry, we added 1 mL of 190 mM sucrose, 1 mM DTT, and 1× protease inhibitor cocktail in 50 mM Tris–HCl, pH 7.0, placed the lid of a Petri dish over the cover glass, and left it undisturbed for 3 h to allow formation of giant proteoliposomes. After formation, we transferred the giant proteoliposomes to a microcentrifuge tube (1.5 mL volume, Eppendorf, Westbury, NY) while taking care not to transfer visible pieces of the agarose film.

2.6. Assessment of P-gp by ATPase activity after reconstitution into giant liposomes

In order to determine the rate of ATP hydrolysis of reconstituted liposomes, we incubated them with 30 μM verapamil (a substrate of P-gp) in the presence and absence of 300 μM vanadate in ATPase assay buffer for 10 min at 37 °C. This ATPase assay buffer contained 50 μM KCl, 5 mM NaN_3, 2 mM EGTA, 10 mM $MgCl_2$, 1 mM DTT, 2 mM ouabain, and 50 mM Tris–HCl, pH 7.5. We used vanadate to inhibit the ATPase activity of P-gp. We started the reaction by adding 5 mM ATP and incubated for 20 min at 37 °C. We terminated the reaction with the addition of SDS solution (0.1 mL of 5% w/v SDS) and quantified the amount of inorganic phosphate released by a sensitive colorimetric reaction as described previously [28]. We recorded the specific activity of the transporter as vanadate-sensitive ATPase activity [28].

2.7. Measurement of P-gp transport rate

We prepared assay solutions at 2× the desired final concentration of magnesium ions, Rho123, and ATP to account for dilution of these molecules when mixed with an equal volume of solution containing giant liposomes. We used a concentration of sorbitol that was isoosmolar to the sucrose solution used to form giant proteoliposomes such that the giant proteoliposomes would settle quickly due to the density difference (see Supporting Information, Fig. S1) with minimal or no swelling or shrinking from water flux across the membrane. Assay solution without ATP consisted of 207 mM sorbitol, 50 mM Tris, pH 7.0, 8 mM $MgCl_2$, and 2 μM Rho123. Assay solution with ATP was the same supplemented with 2 mM ATP. To inhibit the P-gp-mediated transport of Rho123 competitively, we transferred a portion of the solution containing giant proteoliposomes to a separate microcentrifuge tube, added verapamil to a final concentration of 30 μM, and incubated them at room temperature for >15 min before use. Assay solution with inhibitor was the same as assay solution with ATP supplemented with 30 μM verapamil.

For microscopic observation of transport, we punched 5 mm diameter holes in a slab of PDMS (approximately 2 mm thick) and adhered the prepunched PDMS to a cover glass to form wells for viewing giant liposomes. We incubated these wells with 5% milk (w/v nonfat dry milk powder in phosphate buffered saline) to prevent non-specific adsorption that may lead to rupture of giant liposomes on the surface of the glass. After rinsing and drying these wells, we placed 30 μL of assay solution into an observation well, added 30 μL of solution containing giant liposomes, and mixed the contents of the well gently using the pipette. After waiting ~1 min to allow the giant liposomes to settle to the bottom of the well, we focused on a region that contained multiple liposomes and used a confocal microscope (Nikon EZ-C1 software, version 3.20) to capture confocal images at 1 min intervals for 30–60 min using an inverted microscope (Nikon Eclipse TE2000-U) with a 20× objective (Nikon, NA = 0.75) and equipped with an argon laser (Spectra-physics, wavelength = 488 nm), a helium–neon laser (Melles-Griot, wavelength = 543 nm), appropriate filter settings for Rho123, and a pinhole diameter of 33.3 μm.

2.8. Data analysis

We used EZ-C1 viewer (Nikon, version 3.50) to measure the diameter of liposomes and the fluorescence intensity of their interiors, their membranes and the surrounding solution as a function of time. We determined that the fluorescence intensity was linearly related to the concentration of Rho123 in solution (see Supporting Information, Fig. S2). To overcome any experimental variation, we performed a two point calibration before each experiment to determine the Rho123 concentration from fluorescence intensity values using the average intensity inside GUVs without P-gp at the starting time (concentration of Rho123 ~ 0 μM) and the average intensity of the solution outside of GUVs at the starting time (concentration of Rho123 = 1 μM). For the analysis of P_s and k_T, we omitted liposomes that were clearly not unilamellar or that visibly contained small vesicles inside (see Supporting Information, Fig. S5), as well as liposomes whose fluorescence increase did not follow the model represented by Eq. (2) (i.e. $R^2 < 0.9$). The time-dependent fluorescence increase (and hence the increase in Rho123 concentration) of most liposomes could, however, be described very well with Eq. (2) ($R^2 > 0.98$).

We used a non-parametric Kruskal–Wallis test in Origin 8.0 to assess the statistical significance of the data for each experimental condition.

2.9. Patch clamp experiments with proteoliposomes

We placed a 20 μL drop of proteoliposome suspension in the center of a 35 mm glass-bottom Petri dish (MatTek, Ashland, MA) that we had pretreated with 5% milk (w/v dry nonfat milk powder in phosphate buffered saline) for 30 min. Then we covered the dish with 2 mL of

bath solution while taking care to keep the giant proteoliposomes near the center of the dish. Most of the giant proteopliposomes settled to the bottom of the dish within a few minutes. The bath solution consisted of 130 mM KCl, 1 mM $MgCl_2$, and 10 mM HEPES with a pH titrated to 7.2 using KOH. The pipette solution was identical to the bath solution supplemented with 5 mM ATP. We fabricated the patch electrodes with resistances of 5.0–10.0 MΩ from borosilicate glass (Sutter Instruments, Novato, CA) using a P-87 puller (Sutter Instruments, Novato, CA). After formation of a Giga seal, we pulled the patch electrode away from the giant proteoliposome and quickly went through the water–air interface in order to ensure the inside-out configuration. We recorded the single channel current at room temperature using an Axopatch 200B amplifier (Molecular Devices, Sunnyvale, CA) and digitized the recordings using a Digidata 1322A (Molecular Devices, Sunnyvale, CA). The cut-off filter frequency was 5 kHz and the sampling rate was 25 kHz. Data acquisition was done using pClamp9 software (Molecular Devices, Sunnyvale, CA).

3. Results and discussion

3.1. Hydrogel-assisted formation of giant proteoliposomes from small proteoliposomes

We formed giant proteoliposomes that contained P-gp in the phospholipid membrane in three steps by first forming small proteoliposomes with P-gp, second, dehydrating the small proteoliposomes onto a dried film of ultra-low melting agarose, and third, rehydrating the film. Fusion of small proteoliposomes during the swelling of the partially dried hydrogel [4,24,46] readily formed giant liposomes that contained P-gp (Figs. 1A and S4C). Giant liposomes also formed readily from small control liposomes that did not contain P-gp (Figs. 1B and S4A) using the same method. Many of these giant liposomes had diameters larger than 10 μm. Since reconstitution of P-gp into small proteoliposomes has been previously demonstrated to orient the protein in the inside-out orientation [34,42], we hypothesized that at least a fraction of P-gp would reconstitute into giant proteoliposomes in the same inside-out orientation. This hypothesis stems from work by Girard et al. who demonstrated that ~70% of giant proteoliposomes maintained their protein orientation after preparation by alternating electric field-induced fusion of partially dehydrated small proteoliposomes. In other words, fusion of small liposomes with membrane proteins reconstituted in the inside-out configuration led to giant proteoliposomes with a majority of membrane proteins in the same inside-out orientation. Since the hydrogel swelling reported here also induced fusion of previously-formed, partially dehydrated small proteoliposomes with inside-out orientation, we considered a similar bias towards more proteins in the inside-out configuration likely although we cannot rule out a random distribution of orientations or an opposite bias towards a preferred outside-out orientation. The results in Figs. 2 and 3, however, demonstrate that a significant fraction of P-gp proteins were oriented in the inside-out configuration since directional, active transport of Rho123 into the liposomes occurred. In contrast, had all P-gp molecules been oriented in the outside-out orientation, this active transport would not have been significant compared to passive transport. This inward direction of active transport means that the ATP-binding domain of P-gp was accessible on the exterior of the proteoliposomes and that ATP hydrolysis enabled directional transport of Rho123 into the liposomes as expected for the inside-out orientation as opposed to efflux of substrate as naturally occurs in cells when P-gp is oriented outside-out.

To test the functionality of the reconstituted P-gp, we measured the ATPase activity on giant and small proteoliposomes that contain P-gp. We found that stimulation with the well-known P-gp substrate verapamil resulted in a higher level of ATPase activity compared to that observed in the absence of verapamil (see Supporting Information, Table S1). This substrate-induced ATP hydrolysis indicated that a significant fraction of P-gp was measurably active with the ATP-binding domain accessible to the external solution after the process of reconstitution via dried films of ultra-low melting agarose [30,41,42].

3.2. Assessment of protein function using a transport assay

To test for active transport of substrates into giant proteoliposomes by P-gp, we developed a transport assay using a P-gp substrate, rhodamine 123 (Rho123), which is a fluorescent molecule that emits green light [30,32,37,47,48]. The use of larger giant proteoliposomes (>10 μm) in combination with confocal microscopy could be advantageous because,

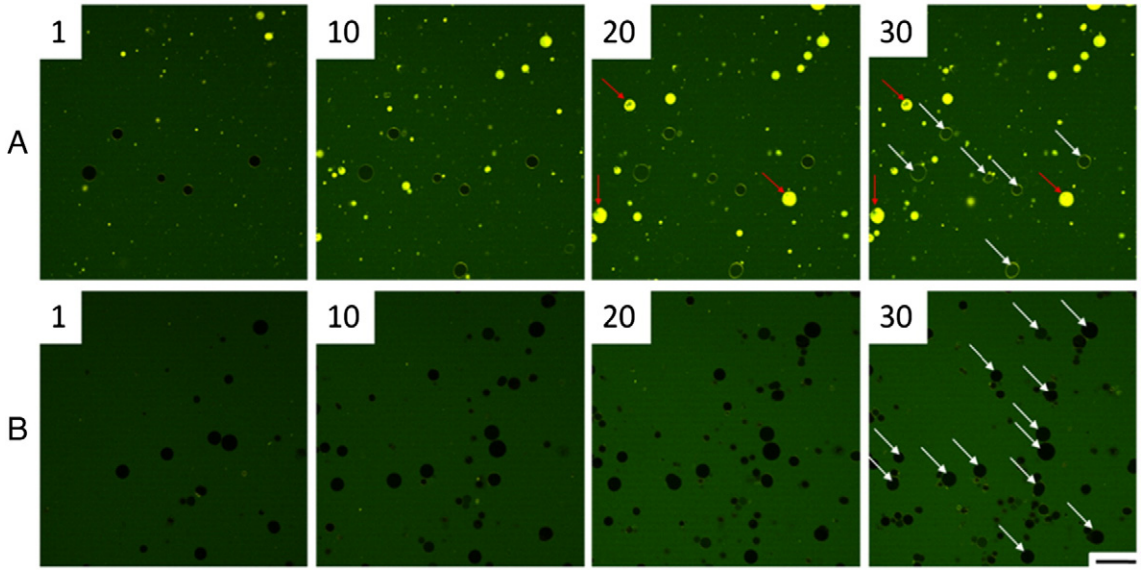

Fig. 1. Confocal microscopy images of giant liposomes with or without reconstituted P-glycoprotein (P-gp) in a solution containing 1 μM of the fluorescent substrate rhodamine 123 (Rho123) and 1 mM ATP. Row A) Giant proteoliposomes formed with P-gp. Row B) Control experiment with giant liposomes that were formed in the same way as the P-gp liposomes but without P-gp in the membrane. Numbers in the upper left corner of each image indicate elapsed time after immersion in Rho123 solution in minutes. The red arrows indicate giant proteoliposomes with an inhomogeneous interior that reveals the presence of small liposomes inside (see also Supporting Information Fig. S5D, E). White arrows indicate proteoliposomes with interiors that exhibited a change in fluorescence intensity over time and were included in the data analysis to obtain permeability coefficients, P_s, and P-gp-induced transport rates, k_T. Scale bar = 100 μm.

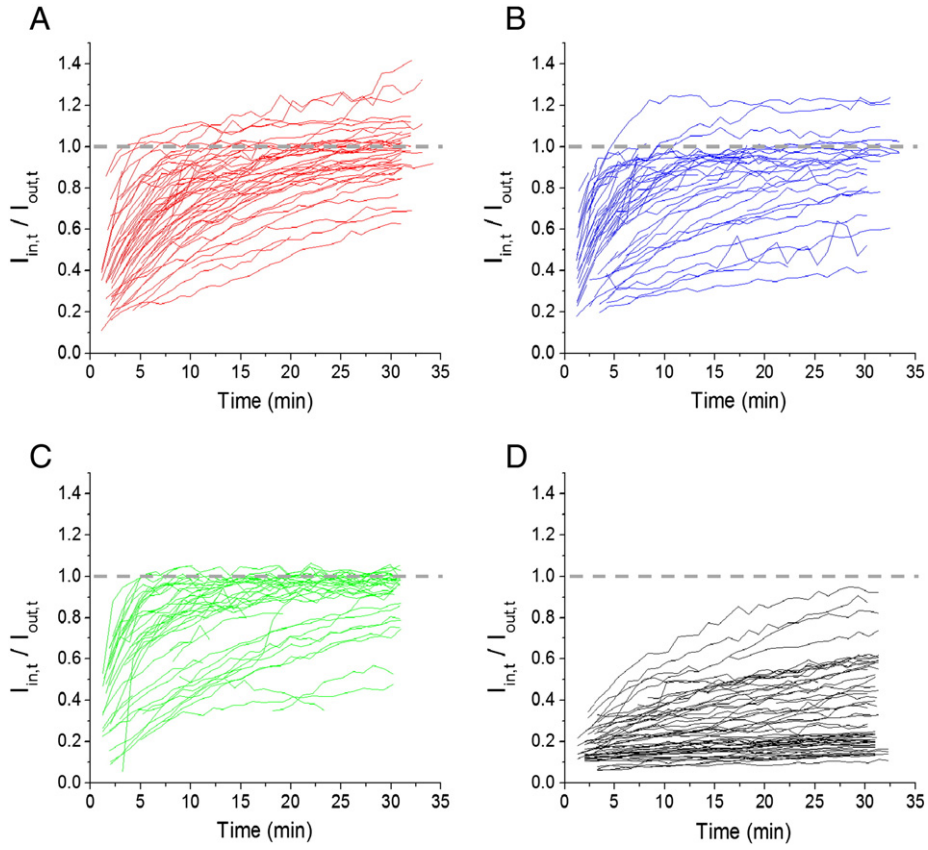

Fig. 2. Time-dependent fluorescence intensity inside giant liposomes ($I_{in,t}$) divided by the fluorescence intensity of the background ($I_{out,t}$). All giant liposomes were assayed in the presence of 1 μM of Rho123. In addition, giant proteoliposomes formed with P-gp were assayed (A) with 1 mM ATP, (B) without ATP, and (C) with 1 mM ATP and 30 μM verapamil and (D) giant proteoliposomes formed without P-gp were assayed with 1 mM ATP. In all graphs "0" time refers to the moment of addition of assay solution (i.e., the start of transport). The dashed gray line shows the level at which the fluorescence intensity inside giant liposomes equals the intensity of the external solution.

in these large GUVs, the internal fluorescence measured near the center of the liposomes is located at a sufficient distance from the liposome membrane, thereby minimizing background signal from membrane-bound fluorescent substrate molecules [2]. These giant proteoliposomes are also straightforward to distinguish individually such that they provide liposome-specific transport data over time [2].

When collecting time-lapse series of fluorescence images following immersion of giant proteoliposomes in a solution containing 1 μM Rho123, we observed a change in fluorescence intensity inside giant proteoliposomes containing P-gp but not in control GUVs that lacked P-gp (Fig. 1). This difference indicated that P-gp was indeed present in the membranes of giant liposomes following the reconstitution process

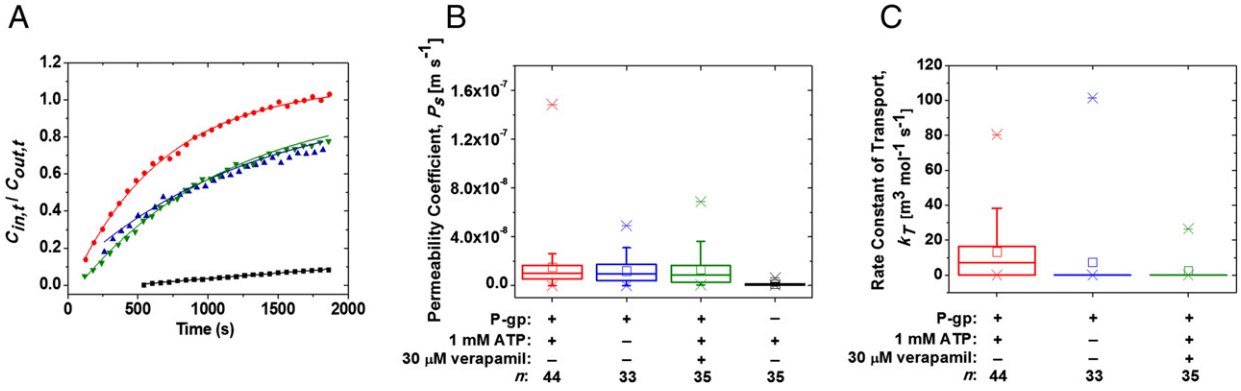

Fig. 3. Determination of membrane permeability, P_s and rate of P-gp-induced active transport, k_T of Rho123. A) Sample data showing the time-dependent concentration of Rho123 inside giant liposomes ($C_{in,t}$) divided by its concentration in the external solution ($C_{out,t}$) and best curve fits of Eq. (2) to the data under four different assay conditions: (●) with P-gp and 1 mM ATP (radius of liposome, $r = 18$ μm, $P_s = 8.8 \times 10^{-9}$ m s^{-1}, $k_T = 9.7$ m^3 mol^{-1} s^{-1}, R^2 of fit = 0.997), (▲) with P-gp but without ATP ($r = 15$ μm, $P_s = 3.9 \times 10^{-9}$ m s^{-1}, $k_T \approx 0$ m^3 mol^{-1} s^{-1}, R^2 of fit = 0.96), (▼) with P-gp, 1 mM ATP and 30 μM verapamil ($r = 16$ μm, $P_s = 4.7 \times 10^{-9}$ m s^{-1}, $k_T \approx 0$ m^3 mol^{-1} s^{-1}, R^2 of fit = 0.99), and ■) Giant liposomes without P-gp ($r = 15$ μm, $P_s = 3.2 \times 10^{-10}$ m s^{-1}, $k_T = 0$ m^3 mol^{-1} s^{-1}, R^2 of fit = 0.99), respectively. Curve fits are shown as solid curves in the corresponding color. B, C) Box plots of experimentally determined distributions of values for the membrane permeability, P_s (B) and rate of P-gp-induced active transport, k_T (C) of Rho123 into giant liposomes under different test conditions. The median P_s values for each condition (from left to right, all in m s^{-1}) were: 9.8×10^{-9}, 9.6×10^{-9}, 8.8×10^{-9}, and 9.9×10^{-10}. The median k_T values for liposomes with P-gp (from left to right, all in m^3 mol^{-1} s^{-1}) were: $k_T = 7.1$, $k_T \approx 0$, and $k_T \approx 0$. The number of liposomes represented in the box plot for each condition is given by n. Symbols in the box plots represent the mean (open square), the median (horizontal line inside the box), the 25th and 75th percentiles (lower and upper bound of the box), the 5th and 95th percentiles (lower and upper whisker), and the 1st and 99th percentiles (lower and upper asterisk).

and thus affected the flux of Rho123 across the membrane. When the fluorescence intensity of the interior started low, we surmised the giant liposome was filled initially with the fluid used to reconstitute the liposome and, therefore, we attributed a time-dependent increase in fluorescence intensity to active transport and passive diffusion of Rho123 from the external solution, across the membrane, and into the internal solution.

During these experiments, we noted a frequent occurrence of bright fluorescent rings in confocal microscopy images of the membranes of giant liposomes containing P-gp (as compared to the background or to the fluorescence of the liposome interior). In contrast, giant liposomes that were generated without P-gp rarely showed these bright fluorescent membranes (Fig. 1). These observations indicate that the difference in membrane fluorescence may be due to the presence of P-gp. Since Rho123 is a substrate of P-gp, one possible explanation for the bright fluorescent membranes could be Rho123 binding to P-gp reconstituted in these membranes. Another possible explanation may be derived from the known accumulation of Rho123 in the lipid membrane [37,47]. Therefore, we speculate that the difference in membrane fluorescence between giant liposomes that did not contain P-gp and proteoliposomes containing P-gp may be due to the presence of P-gp and possible co-reconstituted impurities or due to induced membrane defects from either one of these reconstituted entities, which ultimately enhanced the partitioning of Rho123 in the membrane of these proteoliposomes. We observed bright fluorescent rings with membranes that underwent P-gp reconstitution in both the presence and absence of ATP or verapamil (see Supporting Information, Fig. S4). These results indicate that ATP was not required for Rho123 to associate with P-gp-containing membranes and that the presence of verapamil, a known competitive inhibitor of P-gp-mediated transport of Rho123 [30,32,42,49], was not able to out-compete this association completely.

We also observed the occurrence of liposomes with reconstituted P-gp that reached the fluorescence outside the liposomes within the first few minutes after immersion in Rho123 solution and did not change in fluorescence intensity over time (Fig. 1 and Supporting Information, Fig. S5). These liposomes were present in images of giant proteoliposomes when active transport was enabled (e.g., with ATP) as well as impeded (e.g., without ATP or in the presence of inhibitor) and these liposomes even occurred occasionally, but much less frequently, in preparations that did not contain reconstituted P-gp (see Supporting Information, Fig. S5C). These liposomes were filled with Rho123 most likely due to membrane leakiness or defects (e.g., due to the presence of misfolded P-gp). We also observed brightly fluorescing liposomes with dark circular spots inside, indicating the presence of enclosed regions that contained relatively low concentrations of Rho123 as compared to their surroundings (indicated by red arrows in Figs. 1A, and S5D, E). We attribute these spots to the inclusion of small vesicles [36, 50,51] whose interiors contained relatively low concentration of Rho123 perhaps due to the extra barrier to permeation that their membranes represent or due to their low membrane permeability. The presence of these encapsulated vesicles offers a possible explanation for the fraction of bright fluorescing giant liposomes described above: the close proximity of adjacent membranes may allow membrane-to-membrane transfer (or short diffusion times between membranes) of Rho123 and the subsequent additive membrane reservoir (each of which fluoresces more than background) hence increases the fluorescence intensity inside these multivesicular giant liposomes [36,50,51]. Fig. S5D and E show examples of such liposomes, which were excluded from the data analysis.

To quantify active transport resulting from P-gp, we measured the fluorescence intensity inside the liposomes with respect to the fluorescence intensity outside liposomes (background fluorescence) over time under four different assay conditions: 1) with P-gp and 1 mM ATP, 2) with P-gp but without ATP, 3) with P-gp, 1 mM ATP and 30 μM verapamil to inhibit active transport of Rho123 by P-gp, and 4) without P-gp (Fig. 2). The fluorescence intensity inside giant proteoliposomes formed with P-gp increased quickly in the first 10–15 min after immersion in 1 μM Rho123 assay solution (Fig. 2A), whereas the fluorescence intensity inside giant liposomes without P-gp typically remained low (Fig. 2D). As expected for active transport of Rho123, the fluorescence intensity inside giant proteoliposomes exceeded the intensity of the background fluorescence more often in the presence of 1 mM ATP than without ATP or in the presence of an inhibitor (Fig. 2A). Although we observed the fluorescence intensity inside a few giant proteoliposomes rising higher than the background fluorescence when assayed without ATP (Fig. 2B), these intensities reached a plateau, whereas in the presence of ATP the intensities in many of the proteoliposomes continued to rise (Fig. 2A). Note that Fig. 2A–D shows the raw data without accounting for variations in liposome size. Therefore, individual curves cannot be directly compared with regard to P_s and k_T values of Rho123 influx (see Eq. (2)).

3.3. Model of Rho123 flux that includes passive diffusion and P-gp-mediated active transport

The change in the concentration of Rho123 inside a liposome is due to molecules of Rho123 crossing the membrane into the liposome. Molecules can cross a membrane via passive diffusion in a manner that depends on the difference in concentration on each side of the membrane and a rate constant of diffusion also called the permeability coefficient, P_s ($m\ s^{-1}$), or via active transport in the presence of active transporter proteins that, in the case studied here, depends on the concentration of ATP and a rate constant of transport. In our analysis, we combined the concentration of ATP (which we held constant) and the rate of transport into one variable, k_T ($m^3\ mol^{-1}\ s^{-1}$). Since ATP was added only to the external solution and its diffusion into liposomes was assumed to negligible [52], active transport yielded a net flux from outside to inside the liposome, independent of the concentration of Rho123 inside the liposome. We modeled the change in the concentration of Rho123 in giant liposomes over time t (s) with Eq. (1), which separates the passive transport term [2,53] from the active transport term [54]. The passive transport term stems from Fick's Law and accounts for diffusion across a biological membrane of a spherical liposome with surface area A. The active transport term accounts for the rate of transport as a function of surface density of P-gp and surface area of liposomes. In this equation V is the liposome volume (m^3), C_{in} is the solute concentration of interest ($mol\ m^{-3}$) inside the liposomes, A is the surface area of the liposomes (m^2), ($C_{out} - C_{in}$) is the difference in concentration of solute across the membrane (from external solution to the interior), and Γ_{Pgp} is the surface density of P-gp in the membrane ($mol\ m^{-2}$).

$$V\frac{dC_{in}}{dt} = P_s\,A(C_{out} - C_{in}) + k_T\,\Gamma_{Pgp}\,A\,C_{out} \tag{1}$$

By assuming a constant external concentration of Rho123 surrounding the liposome as well as spherical liposomes with constant volume, integrating Eq. (1) from 0 μM (C_{in} at t_0) to $C_{in,t}$ and from t_0 to t yields Eq. (2),

$$\frac{C_{in}}{C_{out}} = \left(1 - e^{-\frac{3P_S}{r(t-t_0)}}\right)\left(1 + \frac{k_T\Gamma_{Pgp}}{P_S}\right) \tag{2}$$

where r is the measured liposome radius (m) and $3r^{-1}$ is the result of the surface area of a sphere divided by its volume.

We estimated the surface density of P-gp in the membranes of liposomes to be $7.6 \times 10^{-11}\ \frac{mol}{m^2}$, based on the ratio of starting materials (see Supporting Information). We then accounted for possible fluctuations of the fluorescence detection by determining the ratio in concentration between external and internal solutions $\left(\frac{C_{in}}{C_{out}}\right)$ at each time point. Best curve fits of Eq. (2) to this ratio as a function of time determined k_T, P_s and t_0 for each liposome that contained P-gp. Fits to this data from

liposomes that lacked P-gp determined only P_s and t_0 because in this case the surface density of P-gp was zero and no active transport could occur, simplifying Eq. (2) to $\frac{C_{in}}{C_{out}} = 1 - e^{-3P_s/r(t-t_0)}$. Fig. 3A shows sample curves from each of the four assay conditions that show $\frac{C_{in}}{C_{out}}$ as a function of time and the fits of Eq. (2) to these ratios. Due to the assumptions made to estimate the surface concentration of P-gp, the k_T values determined from curve fits are limited to estimates of the active transport rates of P-gp. Nonetheless, we applied various assay conditions to the same batch of liposomes; therefore, these k_T values were useful for comparing the effect of different conditions on the transport rate of P-gp (Fig. 3C). In fact, the median transport rate of P-gp in the absence of ATP or in the presence of inhibitor is very close to zero, indicating that no active transport occurs under these conditions (Fig. 3C).

A non-parametric Kruskal–Wallis test used to compare distributions of P_s and k_T values in Fig. 3B and C revealed that all three conditions of liposomes with reconstituted P-gp had a similar P_s value, whereas liposomes without P-gp had a P_s value that was ~10-fold lower than the liposomes that contained P-gp ($p < 0.05$) (Fig. 3B). These results indicate that the presence of P-gp in the membrane increased the passive membrane permeability of Rho123, even when active transport was not enabled. The median P_s of Rho123 across GUV membranes without P-gp (9.9×10^{-10} m s^{-1}) is approximately one order of magnitude smaller than a previously reported P_s value of Rho123 diffusion across liposome membranes [55] and approximately two orders of magnitude smaller than the P_s value across basolateral membranes of MDCK cells (1×10^{-7} m s^{-1}) [56] as well as the reported P_s values of other known P-gp substrates. For example, P_s values for vincristine, vinblastin, and verapamil across the apical membrane of Caco-2 cells were 3.3×10^{-9}, 1.8×10^{-7}, and 5.2×10^{-6} m s^{-1}, respectively [57]. The low P_s value determined in control liposomes without P-gp suggests that the presence of agarose and association of agarose with the liposomes [24] did not render the liposome membranes leaky to "membrane-impermeable" molecules such as Rho123, as can be seen in the 30 min panel of Fig. 1B. Formation of liposomes from a film of ultra-low melting agarose hence led to giant liposomes with comparable, low-permeability-characteristics than liposomes prepared by other methods [55,58].

With regard to the 10-fold increased P_s value in liposomes with reconstituted proteins, some degree of increased leakiness is commonly observed [39]. The results reported here, however, indicate a strong increase in leakiness in liposomes that underwent reconstitution of P-gp compared to control liposomes without P-gp. We could not differentiate, whether this 10-fold increase in P_s value was due to high local concentration of Rho123 in the P-gp containing membranes, leakiness of the membrane itself (e.g., due to packing defects between lipids in the membrane induced by the nearby presence of P-gp), passage along the surface of P-gp (e.g., via passive transport caused by random changes of P-gp conformation from inward-facing to outward-facing and vice versa) or a combination of these or other effects. We based the choice of lipid for reconstitution on previously reported protocols that have been used to successfully reconstitute functional P-gp into SUVs. One possible reason could be that giant liposomes that underwent P-gp reconstitution interacted more strongly with the glass microscope slides than giant liposomes without P-gp. Such interactions of large proteoliposomes have previously been observed to induce leaks. Despite this unfavorable large leakiness of P-gp containing giant liposomes, the Kruskal–Wallis test nonetheless revealed that the distribution of k_T values for liposomes with active transport (i.e., containing P-gp and assayed with ATP and without verapamil) was significantly higher than the k_T values for liposomes assayed without ATP ($p < 0.05$) or in the presence of verapamil ($p < 0.05$) (Fig. 3C), indicating that active transport could still be differentiated from passive transport or leaks.

Similar to the passive transport, the rate of accumulation of P-gp substrate inside the liposome due to active transport is dependent on the size of the liposome. The observed increase in the values of k_T in the presence of ATP and absence of inhibitor indicates active transport by functional P-gp in the inside-out orientation (Fig. 3C). Additional evidence for active transport stems from the observation that the fluorescence intensity inside the liposomes exceeded the intensity outside the liposomes for several liposomes after assay durations of at least 20 min and continued to increase thereafter, whereas the fluorescence intensity inside liposomes without ATP or with inhibitor reached a plateau at lower levels (Figs. 2 and 3A). These results indicate that functionally active P-gp proteins were reconstituted from small proteoliposomes into giant proteoliposomes via a dried film of ultra-low melting agarose. Furthermore, ATP-mediated transport of Rho123 into giant proteoliposomes demonstrated that a significant fraction of the active P-gp retained their inside-out orientation.

A significant benefit of using giant proteoliposomes for transport analyses is the ability to discern and evaluate vesicles individually. As shown in Eq. (1), the concentration (or number) of molecules transported into the liposome is dependent on the surface area of the vesicle. Methods of generating giant proteoliposomes (as well as small proteoliposomes), however, yield a heterogeneous population with a wide range of sizes. Here we report that a liposome-based transport assay that is simple to perform, yields concentration data of fluorescent substrates with respect to vesicle size, and provides the ability to visually assess individual liposomes for irregularities and artifacts that could affect the influx of substrates. For example, as discussed previously, bright spots inside a fraction of liposomes likely corresponded to multilamellar liposomes or to giant liposomes filled with small vesicles. The presence of such internalized liposomes is not unusual for methods of generating giant liposomes with embedded membrane proteins based on variations of the gentle hydration method [51], but could skew the results when liposomes are too small to discern individually due to the brightness of the membrane fluorescence. The giant proteoliposomes prepared with the method presented here make it possible to exclude such artifacts from the analysis.

3.4. Evaluation of ion channel activity of chloride channels co-purified with P-gp

Previous reports have associated P-gp with chloride channel activity, presumably by co-purification of these channels with P-gp [33,34,59–62]. Therefore, as an additional means of testing the functionality of proteins reconstituted in giant proteoliposomes via the method introduced here, we performed patch clamp experiments employing the inside-out configuration from giant proteoliposomes and compared the current recorded from membranes of GUVs containing P-gp with the current recorded from membranes without P-gp (Fig. 4). These giant proteoliposomes with large diameters (>10 μm) are well suited for performing these experiments.

We observed transient and distinct open and closed states in the patch clamp recordings of membrane patches from giant proteoliposomes that contained P-gp (Fig. 4B). In comparison, patch clamp recordings of membrane patches from GUVs that lacked P-gp but were otherwise formed with the same protocol from a film of agarose did not show current fluctuations beyond baseline noise (Fig. 4A). These results indicate that functional ion channel proteins were reconstituted in giant proteoliposomes when reconstituting the purified P-gp preparation by the method reported here.

To investigate if these ion channel activities originated from chloride channel proteins that co-purified with P-gp from the host insect cells, we applied two well-known chloride channel inhibitors (Fig. S6) and found that channel activity was blocked in the presence of 100 μM of the potent chloride channel inhibitor, 5-nitro-2-(3-phenylpropylamino)benzoic acid (NPPB), but was restored after washing out the inhibitor as expected [63,64]. Channel activity was irreversibly blocked after application of 50 μM Gd^{3+}, as expected for chloride channels [63,65]. The results indicate the presence of chloride channel proteins in giant proteoliposomes containing purified P-gp and agree with previous studies [64,66,67]. For instance,

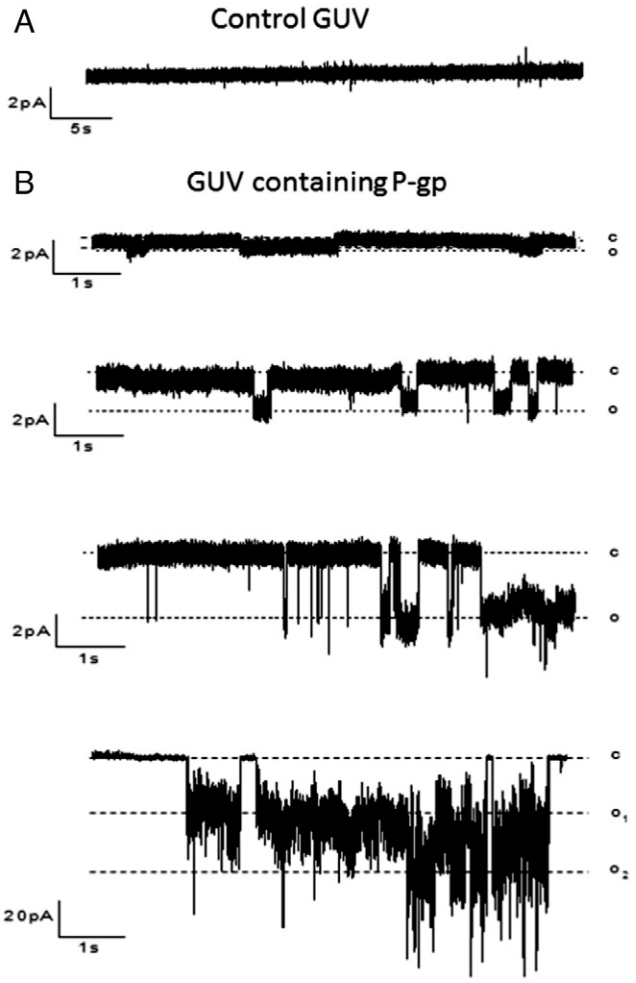

Fig. 4. Patch clamp recordings from giant liposomes formed on an agarose film from small liposomes that contained or did not contain purified P-glycoprotein (P-gp). Single channel currents were recorded after excising a membrane patch from the proteoliposomes in the inside-out configuration at a holding potential of −100 mV. (A) Current trace of single channel recordings from a control GUV without P-gp. (B) Current traces of single channel recordings from giant proteoliposomes with reconstituted purified P-gp. Traces were filtered at 2 kHz. The mean single channel conductance values were (from top to bottom panel): 6, 19, 37, and 245 pS, respectively.

Ehring et al. [64] reported single channel conductance values of 6.1 pS and 25.2 pS from multi-drug resistance cell lines while Duan et al. [67] reported a single channel conductance value of 40 pS. In addition, Schwiebert et al. [66] observed a large conductance chloride channel with a single channel conductance value of 305 pS. Together, these conductance values compare well with the ones obtained from Fig. 4.

3.5. Comparison with a previously described reconstitution method

When choosing a method for reconstituting proteins into giant proteoliposomes, the required properties of the resulting liposomes must be considered. For example, to study ion channels using the traditional, pipette-based patch clamp technique, only a few giant proteoliposomes need to be present because the experimentalist can select a proteoliposome of choice from a heterogeneous population. In addition, the presence of lipid vesicles inside such giant liposomes is of no concern since only the outer liposome membrane is accessed and excised by the patch pipette. For semi-automated, suction-based planar patch clamp assays [68–70], however, a high concentration of unilamellar proteoliposomes with large diameters is desirable to ensure acceptable success rates of bilayer formation over micro- or nanopores [6]. Similarly, the ideal case for fluorescence-based transport assays as described in the work presented here would be an abundance of unilamellar proteoliposomes with diameters larger than 10 μm so that influx of solutes into liposomes can be readily monitored and analyzed using time series of images. Ideally most of these liposomes would not contain other liposomes within them, since the volume excluded by such internalized liposomes may reduce the effective volume of the GUV. To compare the agarose-based method presented here with an existing method for producing giant proteoliposomes, we formed giant liposomes containing P-gp using the gentle hydration method presented by Riquelme et al. [17]. Both methods could produce a similar yield of giant liposomes after collecting free-floating liposomes using a pipette. Formation of giant proteoliposomes using the previously described method of gentle hydration was, however, less reliable (some trials yielded very few free-floating giant proteoliposomes) than the formation from a film of ultra-low melting agarose described here (every trial produced a good yield of giant proteoliposomes). We also found that the previously described method [17] produced liposomes that were more often packed with small liposomes compared to the method presented here (Fig. 5). While these internal liposomes did not interfere with the patch clamp studies performed by Riquelme et al. [17], these types of liposomes were not suitable for transport assays that measure the fluorescence intensity inside liposomes as described here. Therefore, the yield of suitable proteoliposomes for fluorescent flux assays was significantly higher when formation was facilitated by a film of ultra-low melting agarose in comparison to the previously established protocol.

3.6. Evaluation of the lamellarity of the resulting proteoliposomes

We followed a fluorescence-based procedure reported by Akashi et al. to evaluate whether the proteoliposomes prepared by the method

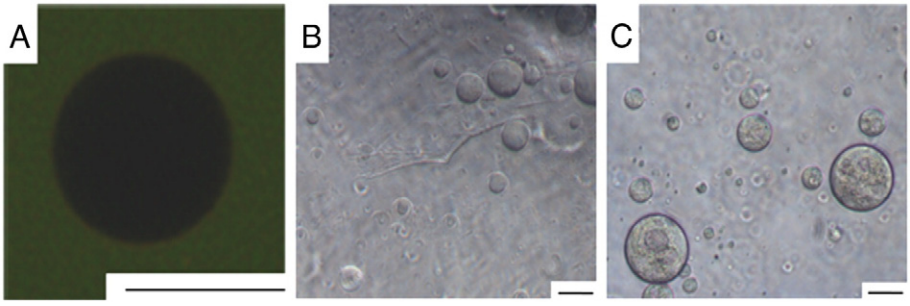

Fig. 5. Confocal and phase contrast images of giant liposomes formed from small proteoliposomes. Small proteoliposomes were dehydrated on a dried film of ultra-low melting agarose before reconstitution in an aqueous solution of 10 mM Tris (pH 7.0), 190 mM sucrose, 1 mM dithiothreitol, and 1× protease inhibitor. After reconstitution, giant proteoliposomes were added to assay solution containing Rho123 and ATP to final concentrations of 1 μM and 1 mM respectively. A) Confocal image of a giant proteoliposome formed by the method reported here. B) Phase contrast image of giant proteoliposomes formed using the method reported here (same as in A, but without assay solution). C) Phase contrast image of giant proteoliposomes formed by following the method reported by Riquelme et al. [17]. Small proteoliposomes were partially dehydrated on bare glass in the presence of 5% (v/v) ethylene glycol. Dehydration of small proteoliposomes was followed by overnight reconstitution in the aqueous solution used in (A and B). Scale bars = 50 μm.

presented here were unilamellar or multilamellar [24,50]. Fig. 6 shows the Rho123-induced membrane fluorescence as a function of proteoliposome diameter as well as the resulting distribution of membrane fluorescence values. The presence of one major peak in the distribution of membrane fluorescence suggests that the majority of proteoliposomes that were used for quantitative flux analysis as defined by the criteria in the Materials and methods section and the main text were unilamellar. We note, however, that these criteria excluded a significant fraction of liposomes that were filled with bright fluorescence and were therefore obviously multilamellar or multivesicular. As exemplified for instance in the 30 min panel of Fig. 1A, only the proteoliposomes indicated by white arrows passed the criteria for quantitative analysis in this particular fluorescent micrograph. Fig. 6 shows that within the fraction that passed the criteria for quantitative analysis, only six of 76 liposomes had magnitudes of membrane fluorescence significantly above the first peak in the distribution and were hence considered multilamellar.

4. Conclusion

Dried films of ultra-low melting agarose facilitated the formation of giant proteoliposomes from small proteoliposomes. The resulting giant proteoliposomes contained purified P-gp transporters and exhibited (i) increased ATPase activity following stimulation with a known transport substrate compared to pre-stimulation activity, (ii) elevated membrane permeabilities to Rho123 in liposomes containing P-gp compared to liposomes lacking P-gp, (iii) elevated rates of transport under conditions conducive to active transport by P-gp compared to conditions without ATP or with an inhibitor, and (iv) single ion channel currents consistent with co-purified chloride channel proteins. Together, these results demonstrate that this technique yielded functional reconstitution of purified transmembrane proteins such as P-gp and chloride ion channels into giant proteoliposomes. At least a fraction of the P-gp proteins remained in the inside-out orientation, wherein the ATP-binding and substrate-binding domains were exposed to the external solution. Unlike cellular assays, this orientation allows straightforward and rapid alteration of the environment surrounding these domains and provides a means of studying direct effects of potential inhibitors and ATP concentration on the rate of transport. Agarose-mediated reconstitution of transmembrane proteins into giant liposomes resulted in a good yield of giant proteoliposomes, which contained a significant fraction of liposomes that were free of internalized vesicles and hence suitable for transport studies and may enable experiments with semi-automated planar patch clamp experiments on reconstituted and purified proteins.

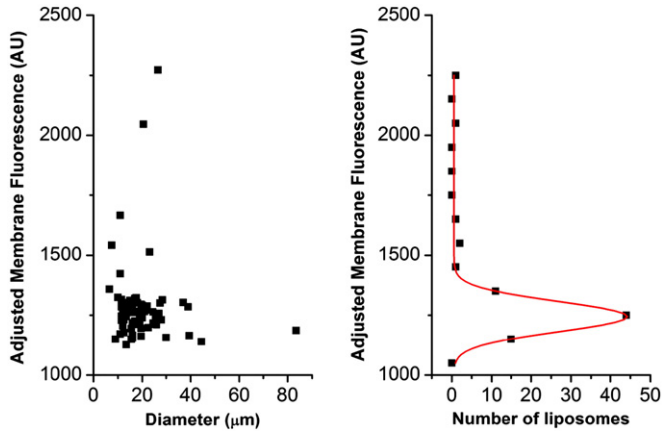

Fig. 6. Adjusted membrane fluorescence from Rho123 as a function of proteoliposome diameter and corresponding distribution of membrane fluorescence values. In this analysis the peak with the lowest membrane fluorescence value (here 1245 AU) is attributed to unilamellar liposomes, while liposomes with significantly higher membrane fluorescence are considered multilamellar [24,50]. Adjusted membrane fluorescence is defined as (intensity of membrane fluorescence) / (intensity of local background fluorescence/average of the intensity of the background fluorescence from all analyzed images).

The major disadvantage of the method presented here was the unexpectedly large flux of Rho123 through the resulting liposomes by passive diffusion in the proteoliposomes with reconstituted P-gp. Since we used a previously published lipid mixture for P-gp reconstitution, we do not know the reason for the 10-fold increased leakiness of membranes containing P-gp compared to the control liposomes without P-gp. It remains to be seen if similar problems of leakiness will appear with reconstituted proteins other than P-gp or if this problem was protein-specific. Recently Lira et al. reported that liposomes, which were also formed from films of agarose and were initially tight, became permeable to solutes upon transient pore formation by electroporation [58]. The authors explained this effect by trapping of agarose molecules in the membrane pores and a resulting attenuation of spontaneous pore closure. As one possible explanation for the increased leakiness upon P-gp reconstitution, we speculate that the presence of P-gp in the membranes may increase the probability of spontaneous pore formation in the liposome membranes whose closure may be impeded by the same agarose-induced mechanism. If this is indeed the case then one variation of our original hydrogel swelling method, namely to use a chemically cross-linked hydrogel (as reported in the Supporting Information of that paper [24]) whose monomers should not be able to dissolve from the hydrogel would be expected to minimize this problem. Moreover, Weinberger et al. [4] and Mora et al. [46] have recently published the formation of giant liposomes from other hydrogels whose monomers are not expected to dissolve from the film. Despite the current shortcomings of the approach presented here, we nonetheless demonstrate that this reconstitution protocol could be used for ion channel recordings with good quality and that a model which considers both passive and active transport by one of the most important multidrug resistance efflux pumps could distinguish between and quantify these two parameters.

Based on the results presented here, we propose that the giant proteoliposomes formed by this reconstitution technique may provide a useful model system for studying the direct effects of potential inhibitors on the rate of active transport by P-gp and potentially other transport or ion channel proteins under well-defined conditions. We expect these systems to aid in drug development and in studying potential interactions of transport proteins with lipids or ion channel proteins.

Acknowledgements

This work was supported by the National Institutes of Health (M.M., grant no. 1R01GM081705) and the Air Force Office of Scientific Research (AFOSR) (M.M. and D.S. grant no. FA9550-12-1-0435). Drs. S. Shukla and S.V. Ambudkar were supported by the Intramural Research Program of the NIH, National Cancer Institute, Center for Cancer Research. K.S.H. acknowledges a Microfluidics in Biomedical Sciences Training Program fellowship from NIH (grant no. T32EB005582 from the National Institute of Biomedical Imaging and Bioengineering at NIH) and a Rackham Engineering Award Fellowship.

Appendix A. Supplementary data

Calibration curves of osmolarity and density for solutions of sucrose and sorbitol, calibration curve of concentration to fluorescence intensity, purification of P-gp, ATPase assay, fluorescence of GUVs containing P-gp, estimate of the number of proteins per liposome, and inhibition of chloride channel reconstituted in GUVs with P-gp. Supplementary data associated with this article can be found, in the online version, at http://dx.doi.org/10.1016/j.bbamem.2014.10.023.

References

[1] P.L. Luisi, P. Walde, Perspectives in supramolecular chemistry: giant vesicles, in: P.L. Luisi, P. Walde (Eds.), Perspectives in Supramolecular Chemisty: Giant Vesicles, vol. 6, John Wiley & Sons, New York, 2000, pp. 1–426.

[2] S. Li, P.C. Hu, N. Malmstadt, Confocal imaging to quantify passive transport across biomimetic lipid membranes, Anal. Chem. 82 (2010) 7766–7771.
[3] B. Maherani, E. Arab-Tehrany, M.R. Mozafari, C. Gaiani, M. Linder, Liposomes: a review of manufacturing techniques and targeting strategies, Curr. Nanosci. 7 (2011) 436–452.
[4] A. Weinberger, F.-C. Tsai, Gijsje H. Koenderink, Thais F. Schmidt, R. Itri, W. Meier, T. Schmatko, A. Schröder, C. Marques, Gel-assisted formation of giant unilamellar vesicles, Biophys. J. 105 (2013) 154–164.
[5] L.A. Bagatolli, D. Needham, Quantitative optical microscopy and micromanipulation studies on the lipid bilayer membranes of giant unilamellar vesicles, Chem. Phys. Lipids 181 (2014) 99–120.
[6] L. Tiefenauer, S. Demarche, Challenges in the development of functional assays of membrane proteins, Materials 5 (2012) 2205–2242.
[7] P. Walde, K. Cosentino, H. Engel, P. Stano, Giant vesicles: preparations and applications, Chembiochem 11 (2010) 848–865.
[8] M. Dezi, A. Di Cicco, P. Bassereau, D. Levy, Detergent-mediated incorporation of transmembrane proteins in giant unilamellar vesicles with controlled physiological contents, Proc. Natl. Acad. Sci. U. S. A. 110 (2013) 7276–7281.
[9] S. Aimon, J. Manzi, D. Schmidt, J.A.P. Larrosa, P. Bassereau, G.E.S. Toombes, Functional reconstitution of a voltage-gated potassium channel in giant unilamellar vesicles, PLoS One 6 (2011) e25529.
[10] Y.J. Liu, G.P.R. Hansen, A. Venancio-Marques, D. Baigl, Cell-free preparation of functional and triggerable giant proteoliposomes, Chembiochem 14 (2013) 2243–2247.
[11] J.P. Reeves, R.M. Dowben, Formation and properties of thin-walled phospholipid vesicles, J. Cell. Physiol. 73 (1969) 49–60.
[12] M.I. Angelova, D.S. Dimitrov, Liposome electroformation, Faraday Discuss. 81 (1986) 303–311.
[13] N.F. Morales-Penningston, J. Wu, E.R. Farkas, S.L. Goh, T.M. Konyakhina, J.Y. Zheng, W.W. Webb, G.W. Feigenson, GUV preparation and imaging: minimizing artifacts, Biochim. Biophys. Acta, Biomembr. 1798 (2010) 1324–1332.
[14] P.M. Shaklee, S. Semrau, M. Malkus, S. Kubick, M. Dogterom, T. Schmidt, Protein incorporation in giant lipid vesicles under physiological conditions, Chembiochem 11 (2010) 175–179.
[15] P. Girard, J. Pecreaux, G. Lenoir, P. Falson, J.L. Rigaud, P. Bassereau, A new method for the reconstitution of membrane proteins into giant unilamellar vesicles, Biophys. J. 87 (2004) 419–429.
[16] B.U. Keller, R. Hedrich, W.L. Vaz, M. Criado, Single channel recordings of reconstituted ion channel proteins: an improved technique, Pflugers Arch. 411 (1988) 94–100.
[17] G. Riquelme, E. Lopez, L.M. Garcia-Segura, J.A. Ferragut, J.M. Gonzalez-Ros, Giant liposomes: a model system in which to obtain patch-clamp recordings of ionic channels, Biochemistry 29 (1990) 11215–11222.
[18] M.K. Doeven, J.H.A. Folgering, V. Krasnikov, E.R. Geertsma, G. van den Bogaart, B. Poolman, Distribution, lateral mobility and function of membrane proteins incorporated into giant unilamellar vesicles, Biophys. J. 88 (2005) 1134–1142.
[19] A.R. Battle, E. Petrov, P. Pal, B. Martinac, Rapid and improved reconstitution of bacterial mechanosensitive ion channel proteins MscS and MscL into liposomes using a modified sucrose method, FEBS Lett. 583 (2009) 407–412.
[20] M. Yanagisawa, M. Iwamoto, A. Kato, K. Yoshikawa, S. Oiki, Oriented reconstitution of a membrane protein in a giant unilamellar vesicle: experimental verification with the potassium channel KcsA, J. Am. Chem. Soc. 133 (2011) 11774–11779.
[21] N. Kahya, E.I. Pecheur, W.P. de Boeij, D.A. Wiersma, D. Hoekstra, Reconstitution of membrane proteins into giant unilamellar vesicles via peptide-induced fusion, Biophys. J. 81 (2001) 1464–1474.
[22] A. Varnier, F. Kermarrec, I. Blesneac, C. Moreau, L. Liguori, J.L. Lenormand, N. Picollet-D'hahan, A simple method for the reconstitution of membrane proteins into giant unilamellar vesicles, J. Membr. Biol. 233 (2010) 85–92.
[23] D.J. Estes, S.R. Lopez, A.O. Fuller, M. Mayer, Triggering and visualizing the aggregation and fusion of lipid membranes in microfluidic chambers, Biophys. J. 91 (2006) 233–243.
[24] K.S. Horger, D.J. Estes, R. Capone, M. Mayer, Films of agarose enable rapid formation of giant liposomes in solutions of physiologic ionic strength, J. Am. Chem. Soc. 131 (2009) 1810–1819.
[25] J.S. Hansen, J.R. Thompson, C. Helix-Nielsen, N. Malmstadt, Lipid directed intrinsic membrane protein segregation, J. Am. Chem. Soc. 135 (2013) 17294–17297.
[26] M.G. Gutierrez, N. Malmstadt, Human serotonin receptor 5-HT1A preferentially segregates to the liquid disordered phase in synthetic lipid bilayers, J. Am. Chem. Soc. 136 (2014) 13530–13533.
[27] S.V. Ambudkar, C.O. Cardarelli, I. Pashinsky, W.D. Stein, Relation between the turnover number for vinblastine transport and for vinblastine-stimulated ATP hydrolysis by human P-glycoprotein, J. Biol. Chem. 272 (1997) 21160–21166.
[28] S.V. Ambudkar, Drug-stimulatable ATPase activity in crude membranes of human MDR1-transfected mammalian cells, Abc Transporters: Biochemical, Cellular, and Molecular Aspects, 2921998. 504–514.
[29] S.V. Ambudkar, C. Kimchi-Sarfaty, Z.E. Sauna, M.M. Gottesman, P-glycoprotein: from genomics to mechanism, Oncogene 22 (2003) 7468–7485.
[30] F.J. Sharom, The P-glycoprotein multidrug transporter, in: F.J. Sharom (Ed.), Essays in Biochemistry: Abc Transporters, vol. 50, Portland Press Ltd, London, 2011, pp. 161–178.
[31] A. Palmeira, E. Sousa, M.H. Vasconcelos, M.M. Pinto, Three decades of P-gp inhibitors: skimming through several generations and scaffolds, Curr. Med. Chem. 19 (2012) 1946–2025.
[32] C. Ramachandran, S.J. Melnick, Multidrug resistance review in human tumors — molecular diagnosis and clinical significance, Mol. Diagn. 4 (1999) 81–94.
[33] P.R. Wielinga, N. Heijn, H.V. Westerhoff, J. Lankelma, A method for studying plasma membrane transport with intact cells using computerized fluorometry, Anal. Biochem. 263 (1998) 221–231.
[34] E.M. Howard, P.D. Roepe, Purified human MDR 1 modulates membrane potential in reconstituted proteoliposomes, Biochemistry 42 (2003) 3544–3555.
[35] M.K. Al-Shawi, H. Omote, The remarkable transport mechanism of P-glycoprotein: a multidrug transporter, J. Bioenerg. Biomembr. 37 (2005) 489–496.
[36] K. Bucher, S. Belli, H. Wunderli-Allenspach, S.D. Kramer, P-glycoprotein in proteoliposomes with low residual detergent: the effects of cholesterol, Pharm. Res. 24 (2007) 1993–2004.
[37] H. Sasaki, R. Kawano, T. Osaki, K. Kamiya, S. Takeuchi, Single-vesicle estimation of ATP-binding cassette transporters in microfluidic channels, Lab Chip 12 (2012) 702–704.
[38] S.P. Hardy, H.R. Goodfellow, M.A. Valverde, D.R. Gill, F.V. Sepulveda, C.F. Higgins, Protein-kinase C-mediated phosphorylation of the human multidrug-resistance P-glycoprotein regulates cell volume-activated chloride channels, EMBO J. 14 (1995) 68–75.
[39] R.B. Gennis, Biomembranes: Molecular Structure and Function, Springer-Verlag, New York, 1989.
[40] M. Ramachandra, S.V. Ambudkar, D. Chen, C.A. Hrycyna, S. Dey, M.M. Gottesman, I. Pastan, Human P-glycoprotein exhibits reduced affinity for substrates during a catalytic transition state, Biochemistry 37 (1998) 5010–5019.
[41] W. Schaffner, C. Weissman, Rapid, sensitive, and specific method for determination of protein in dilute-solution, Anal. Biochem. 56 (1973) 502–514.
[42] S.V. Ambudkar, I.H. Lelong, J.P. Zhang, C.O. Cardarelli, M.M. Gottesman, I. Pastan, Partial-purification and reconstitution of the human multidrug-resistance pump — characterization of the drug-stimulatable ATP hydrolysis, Proc. Natl. Acad. Sci. U. S. A. 89 (1992) 8472–8476.
[43] S.V. Ambudkar, P.C. Maloney, Anion-exchange in bacteria — reconstitution of phosphate–hexose 6-phosphate antiport from streptococcus-lactis, Methods Enzymol. 125 (1986) 558–563.
[44] P.C. Maloney, S.V. Ambudkar, Functional reconstitution of prokaryote and eukaryote membrane-proteins, Arch. Biochem. Biophys. 269 (1989) 1–10.
[45] S.V. Ambudkar, I.H. Lelong, J.P. Zhang, C. Cardarelli, Purification and reconstitution of human P-glycoprotein, Abc Transporters: Biochemical, Cellular, and Molecular Aspects, 1998, pp. 492–504.
[46] N.L. Mora, J.S. Hansen, Y. Gao, A.A. Ronald, R. Kieltyka, N. Malmstadt, A. Kros, Preparation of size tunable giant vesicles from cross-linked dextran(ethylene glycol) hydrogels, Chem. Commun. 50 (2014) 1953–1955.
[47] A.B. Shapiro, V. Ling, Stoichiometry of coupling of rhodamine 123 transport to ATP hydrolysis by P-glycoprotein, Eur. J. Biochem. 254 (1998) 189–193.
[48] W. Chearwae, S. Anuchapreeda, K. Nandigama, S.V. Ambudkar, P. Limtrakul, Biochemical mechanism of modulation of human P-glycoprotein (ABCB1) by curcumin I, II, and III purified from Turmeric powder, Biochem. Pharmacol. 68 (2004) 2043–2052.
[49] S. Shukla, C.P. Wu, S.V. Ambudkar, Development of inhibitors of ATP-binding cassette drug transporters — present status and challenges, Expert Opin. Drug Metab. Toxicol. 4 (2008) 205–223.
[50] K. Akashi, H. Miyata, H. Itoh, K. Kinosita, Preparation of giant liposomes in physiological conditions and their characterization under an optical microscope, Biophys. J. 71 (1996) 3242–3250.
[51] N. Rodriguez, F. Pincet, S. Cribier, Giant vesicles formed by gentle hydration and electroformation: a comparison by fluorescence microscopy, Colloids Surf. B: Biointerfaces 42 (2005) 125–130.
[52] A. Petkau, W.S. Chelack, Model lipid membrane permeability to ATP, Can. J. Biochem. 50 (1972) 615–619.
[53] A.C. Chakrabarti, D.W. Deamer, Permeability of lipid bilayers to amino-acids and phosphate, Biochim. Biophys. Acta 1111 (1992) 171–177.
[54] S. Michelson, D. Slate, A mathematical-model of the P-glycoprotein pump as a mediator of multidrug resistance, Bull. Math. Biol. 54 (1992) 1023–1038.
[55] K. Gradauer, S. Duennhaupt, C. Vonach, H. Szoelloesi, I. Pali-Schoell, H. Mangge, E. Jensen-Jarolim, A. Bernkop-Schnuerch, R. Prassl, Thiomer-coated liposomes harbor permeation enhancing and efflux pump inhibitory properties, J. Control. Release 165 (2013) 207–215.
[56] F.X. Tang, O.Y. Hui, J.Z. Yang, R.T. Borchardt, Bidirectional transport of rhodamine 123 and Hoechst 33342, fluorescence probes of the binding sites on P-glycoprotein, across MDCK-MDR1 cell monolayers, J. Pharm. Sci. 93 (2004) 1185–1194.
[57] S. Doppenschmitt, H. Spahn-Langguth, C.G. Regardh, P. Langguth, Role of P-glycoprotein-mediated secretion in absorptive drug permeability: an approach using passive membrane permeability and affinity to P-glycoprotein, J. Pharm. Sci. 88 (1999) 1067–1072.
[58] R.B. Lira, R. Dimova, K.A. Riske, Giant unilamellar vesicles formed by hybrid films of agarose and lipids display altered mechanical properties, Biophys. J. 107 (2014) 1609–1619.
[59] C.F. Higgins, P-glycoprotein and cell volume-activated chloride channels, J. Bioenerg. Biomembr. 27 (1995) 63–70.
[60] M.A. Valverde, M. Diaz, F.V. Sepulveda, D.R. Gill, S.C. Hyde, C.F. Higgins, Volume-regulated chloride channels associated with the human multidrug-resistance P-glycoprotein, Nature 355 (1992) 830–833.
[61] R.W. Johnstone, A.A. Ruefli, M.J. Smyth, Multiple physiological functions for multidrug transporter P-glycoprotein? Trends Biochem. Sci. 25 (2000) 1–6.
[62] T. Mizutani, M. Masuda, E. Nakai, K. Furumiya, H. Togawa, Y. Nakamura, Y. Kawai, K. Nakahira, S. Shinkai, K. Takahashi, Genuine functions of P-glycoprotein (ABCB1), Curr. Drug Metab. 9 (2008) 167–174.
[63] A.D. de Tassigny, R. Souktani, B. Ghaleb, P. Henry, A. Berdeaux, Structure and pharmacology of swelling-sensitive chloride channels, I-Cl, I-swell, Fundam. Clin. Pharmacol. 17 (2003) 539–553.
[64] G.R. Ehring, Y.V. Osipchuk, M.D. Cahalan, Swelling-activated chloride channels in multidrug-sensitive and multidrug-resistant cells, J. Gen. Physiol. 104 (1994) 1129–1161.

[65] M. Suzuki, T. Morita, T. Iwamoto, Diversity of Cl-channels, Cell. Mol. Life Sci. 63 (2006) 12–24.
[66] E.M. Schwiebert, J.W. Mills, B.A. Stanton, Actin-based cytoskeleton regulates a chloride channel and cell-volume in a renal cortical collecting duct cell-line, J. Biol. Chem. 269 (1994) 7081–7089.
[67] D. Duan, C. Winter, S. Cowley, J.R. Hume, B. Horowitz, Molecular identification of a volume-regulated chloride channel, Nature 390 (1997) 417–421.
[68] S. Demarche, K. Sugihara, T. Zambelli, L. Tiefenauer, J. Voros, Techniques for recording reconstituted ion channels, Analyst 136 (2011) 1077–1089.
[69] A. Bruggemann, S. Stoelzle, M. George, J.C. Behrends, N. Fertig, Microchip technology for automated and parallel patch-clamp recording, Small 2 (2006) 840–846.
[70] C. Schmidt, M. Mayer, H. Vogel, A chip-based biosensor for the functional analysis of single ion channels, Angew. Chem. Int. Ed. 39 (2000) 3137–3140.